The importance of temperature control during crystallization and wafering in silicon solar cell production

K. Gastinger, **M. M'Hamdi**, **T. Bergstrøm** & **L. Johnsen**, SINTEF, Trondheim, Norway

This paper first appeared in the seventh print edition of *Photovoltaics International* journal.

ABSTRACT

Heat transfer and control of the temperature field are important in the production of silicon solar cell wafers. Present work focuses on the first steps of the production chain, i.e. crystallization and wafering. For the crystallization process, control of heat transfer is crucial for the ingot quality in terms of grain structure, impurity distribution, particle formation, and ingot stresses. Heat transfer is also important during subsequent processes, in particular the wire sawing of the silicon blocks into wafers. The paper emphasises the role of heat transfer and explains the consequences for these processes. Examples from experimental trials and measurements are combined with models and simulation methods.

Introduction

Wafer-based silicon solar cell production has today the largest market share in the photovoltaic solar energy industry. Crystallization of silicon in the form of ingots is to a large extent carried out either by directional crystallization or the Czochralski (Cz) growth process. Cutting of bulk silicon into wafers is almost exclusively done by sawing of Si-blocks in multi-wire saws.

Control of the heat transfer conditions and the thermal field is important throughout the whole production chain of solar cells. However, the importance of temperature along the production chain varies. Fig. 1 shows the most important process steps for the production of wafers. The colour of the frame depicts the importance of temperature for the process, ranked according to the influence on the wafer quality.

Ingot crystallization and wafer sawing are the process steps with the highest sensitivity to temperature variations and will be discussed in more detail later. Some importance is given to the feedstock melting phase where the high temperatures must be reached. Note that a too long melting and holding period combined with high temperatures prior to crystallization can lead to higher impurity transfer between the ingot and crucible. During block sawing the produced heat can lead to thermally-induced stresses which in addition to the sawing forces can contribute to the initiation and propagation of cracks in particular from the saw damages into the block. Therefore, the sawing speed needs to be adapted. Given that the side surfaces of the block are often grinded and polished to remove saw damages, subsequent processes such as washing/cleaning, singulation, quality control, and sorting/packing are less sensitive to normal temperature variations.

"Control of the heat transfer conditions and the thermal field is important throughout the whole production chain of solar cells."

Temperature measurements are often challenging because of the harsh environment during crystallization and wafer wire sawing processes in particular. Thermal measurements can only be carried out in selected positions, which makes it necessary to combine measurements and modelling to investigate the transient temperature fields. On the other hand, temperature measurements can be used to verify the models.

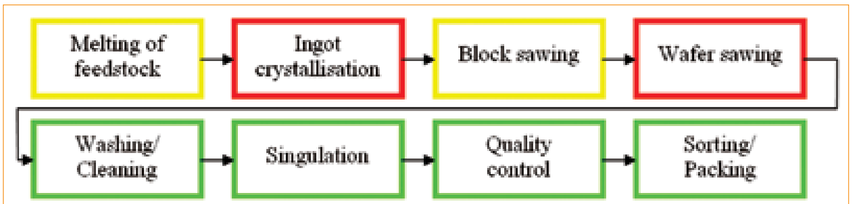

Figure 1. Main processes of the production chain in crystallization and wafering of Si solar cells (red – temperature critical; yellow – temperature moderate critical; green –temperature uncritical).

The most applied point measurement sensors are thermocouples, thermistors, resistance temperature detectors and pyrometers. Optical fibre sensors (Bragg gratings) can supply multipoint measurements along the fibre location. The most widely used method to measure the thermal field of a scene is IR imaging, which records the radiation emitted from the object of interest in the wavelength ranges 3-5μm (MWIR) or 7-14μm (LWIR). The advantages of this optical method are non-contact measurements and the ability to measure spatial distributed temperature fields within 'one shot.'

Simulation tools, in particular heat transfer models, are now available and widely used in the industry to simulate temperature fields e.g. in crystallization furnaces and during wafer wire sawing. The use of these tools is crucial during the design and optimization phases as they provide the opportunity for in-depth understanding of the process and reduce the need for costly trial-and-error approaches. For these models, the boundary conditions are crucial and it is often necessary to measure these parameters with the measuring techniques mentioned earlier.

The following two sections present in more detail the influence of temperature on the two most critical processes: crystallization of the ingot and wire sawing of the block. Models and in-situ measurements are introduced to investigate the influence of temperature fields and optimize the processes.

Crystallization

The control of the thermal field and the crystallization conditions during the silicon casting process is essential for ingot quality as many of the material properties are obtained at this stage of the process chain. Crystallization in furnaces applying directional solidification

(Bridgman) or the Czochralski process, for example, includes all heat transfer phenomena: conduction in solid parts, convection in the melt and the gas phases in addition to radiation (see Fig. 2). Due to the high temperature involved in the process, radiative transfers are the main mechanism for energy transfers in the furnace, e.g. between the heaters and other components, between the crucible support and the cooling plates, or the ingot and the furnace chamber walls.

Heat transfer and phase change

In order to better understand the crystallization process, analysis of the heat balance at the melt-solid interface can be useful:

$$\lambda_s \frac{\partial T_{sol}}{\partial n} - \lambda_l \frac{\partial T_{liq}}{\partial n} = \rho_s L V \qquad (1)$$

where T denotes the temperature, λ the thermal conductivity, n the interface normal direction and ρ_s the density in the solid. Equation 1 reveals that the latent heat of crystallization (L) has to be removed through the solid phase and that the crystallization rate (V) is proportional to the difference between the thermal gradients at the solid-liquid interface. The interface growth rate or the pull speed in the case of the Cz process can be increased by increasing the thermal gradient in the solid and decreasing thermal gradients in the melt. The latter can, for example, be achieved through increased convection in the melt. Control of the temperature field and melt flow in the furnaces of industrial processes is a challenge. Due to the complexity of the transfer phenomena, the use of modelling tools is useful for process analysis and optimization [1,2].

Control of the thermal gradients during the initial stages of multicrystalline silicon crystallization is also quite important for the nucleation and growth conditions at the crucible surface. Experimental studies [3,4] have shown that encouraging dendritic growth at the initial stages of crystallization though the application of high cooling rates can result in fewer grains in the ingot. This reduces extended defects, such as grain boundaries, which is known to be beneficial for the solar cell's efficiency.

Melt and gas flow

During directional solidification processes, the flow field is not very intense and laminar flow conditions can be encountered. Nonetheless, convective transfers are important for the heat transfers and in particular for the planarity of the solid-melt interface (Fig. 2(a)) and should not be neglected in modelling studies [5]. Fig. 3 shows an example of the computed flow field in a small crystallization furnace. For the Cz process, flow phenomena are quite complex due to turbulence. The flow field and thermal gradients in the melt can be influenced through crucible and ingot counter rotations (Fig. 2(b)). In many applications, an electromagnetic field is employed to dump turbulence in the melt and control the thermal field [6]. One should also note that in contrast to directional crystallization, the contribution from Marangoni convection can be quite important in the Cz process. Gas flow does not contribute considerably to the heat transfers in the furnaces but it can affect the flow pattern due to shear stresses at the melt-gas interface and is important for the evaporation and transport of impurities.

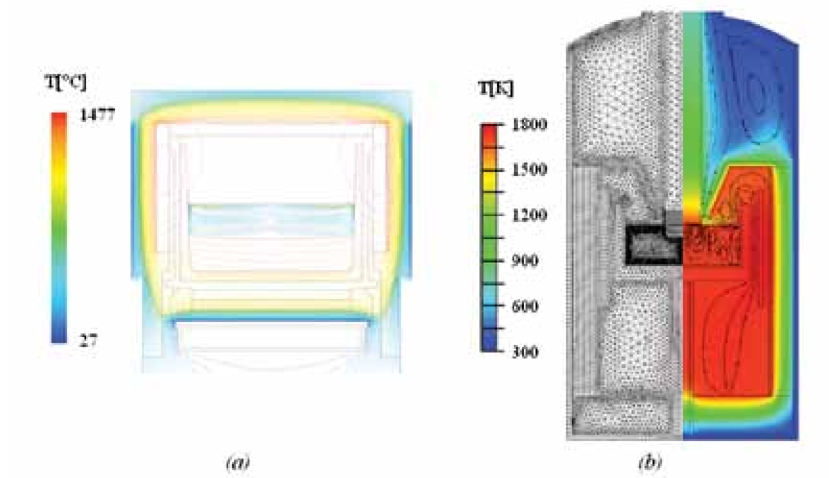

Figure 2. Simulated thermal and flow field for (a) directional crystallization and (b) the Cz process for single crystal growth [1,2].

Impurity transfers

Silicon melt flow and convection in the gas phase are very important for the transfer of impurities and therefore for the ingot quality. The impurity level depends on the quality of the feedstock. Segregation at the solid-liquid interface and convective transfer lead to variations in the impurity concentration throughout the ingot. For many impurities, the use of the Scheil equation provides a good estimate for the segregation profile. For impurities with a low partition coefficient, e.g. metallic impurities, crystallization is a quite efficient refinement process. High temperature (back) diffusion processes during the cooling phase can, however, reduce its efficiency. The furnace usually contains graphite elements to control the heating and the cooling process, while the crucible material may contain impurities such as oxygen and is usually coated with silicon nitride. Contamination from the crucible and interaction with the furnace atmosphere (e.g. oxygen evaporation) leads to the transfer of impurities from and into the silicon melt. When solubility limits are reached, precipitation of silicon carbides and silicon nitrides may occur. The control of the heat transfer and thermal field can lead to quite different flow patterns which in turn can transport impurities towards the ingot centre or to its periphery (Fig. 3) – the latter is more preferable as these regions will be removed as side cuts [7]. Particles formed during the crystallization process are known to have a negative impact on subsequent processes such wafer wire sawing.

Stresses and deformations

Although increasing thermal gradients in the solid phase results in higher growth rates, the consequence is non-uniform cooling conditions that lead to the generation of stresses and deformations in the crystallizing ingot. Even though silicon is brittle for temperatures below 600°C, it is ductile at high temperatures. In this range, thermally-induced deformations are relaxed by

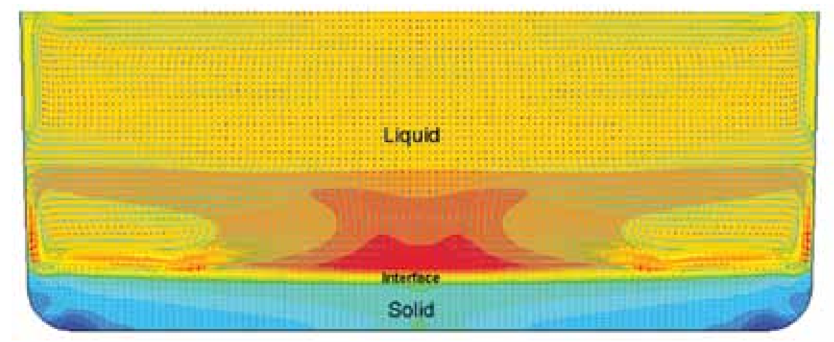

Figure 3. Velocity vectors overlaid with boron concentration (colour scale form 0.8 C0 – blue to 1.09 C0 – red). Typical boron concentration in lower circulation is 1.07 C0 while in upper circulation it is 1.02 C0 [7].

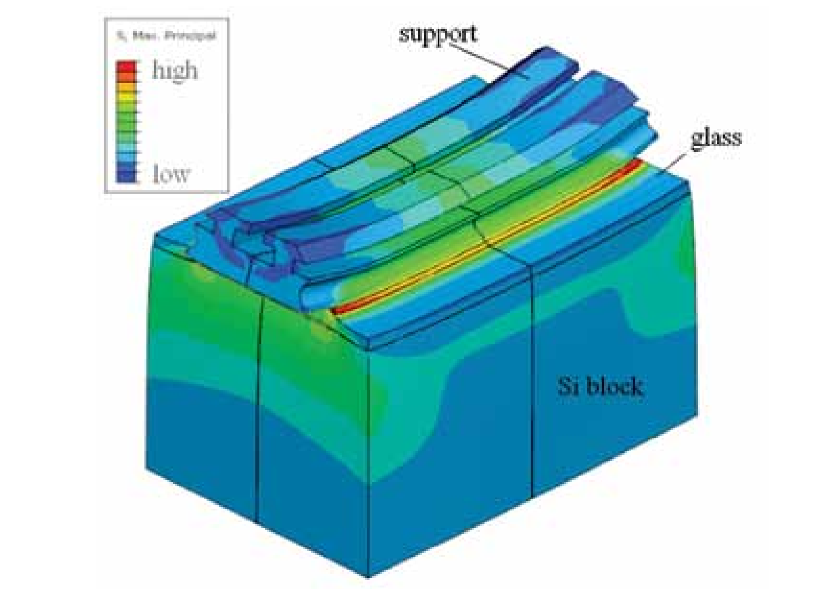

Figure 4. Computed maximal principal stresses in the silicon block after the gluing process. The deformation of the different materials is magnified.

viscoplastic deformation which contributes to dislocation generation and multiplication [8]. Note that plastic relaxation occurs during both the crystallization and the cooling phases. Knowledge of the mechanical properties of silicon at high temperatures is, therefore, important for optimizing the cooling conditions.

Control of the thermal gradient in single crystal ingots and reducing interface deflection are crucial for achieving dislocation and defect-free ingots. For multicrystalline silicon, it is important to recognise that in addition to macroscopic thermal gradients, different relative orientations of the grains lead to stress concentrations at grain boundaries, which may contribute to the generation of dislocation clusters. Note also that particles and precipitates can also lead to high short-range stresses due the mismatch in thermal expansion coefficient compared to the silicon matrix. Because of all these factors, residual stresses will build up in the ingot upon cooling to room temperature. The intensity of the latter is dependent on cooling conditions and the interactions with the crucible. Due to surface defects, it is generally preferable to achieve compressive stresses in the periphery of the ingot rather than tensile stresses to avoid fracture. In some conditions, ingot cracking may occur when ingots are removed from the furnace or during block cutting.

Wafer sawing

The sawing of Si wafers from a block is mainly carried out in multi-wire saws. Even though the first approaches to diamond-coated wire sawing are emerging to the market, the dominant technology is slurry-based sawing with silicon carbide (SiC) particles in a solution with polyethylene glycol (PEG).

Temperature is a critical factor in this process. The wire-sawing process is complex and not yet fully understood. The saw parameters used in industrial production are often based on the experience of the operators. Only sophisticated models can be used to predict the process parameters theoretically, e.g. elastohydrodynamic models [9,10].

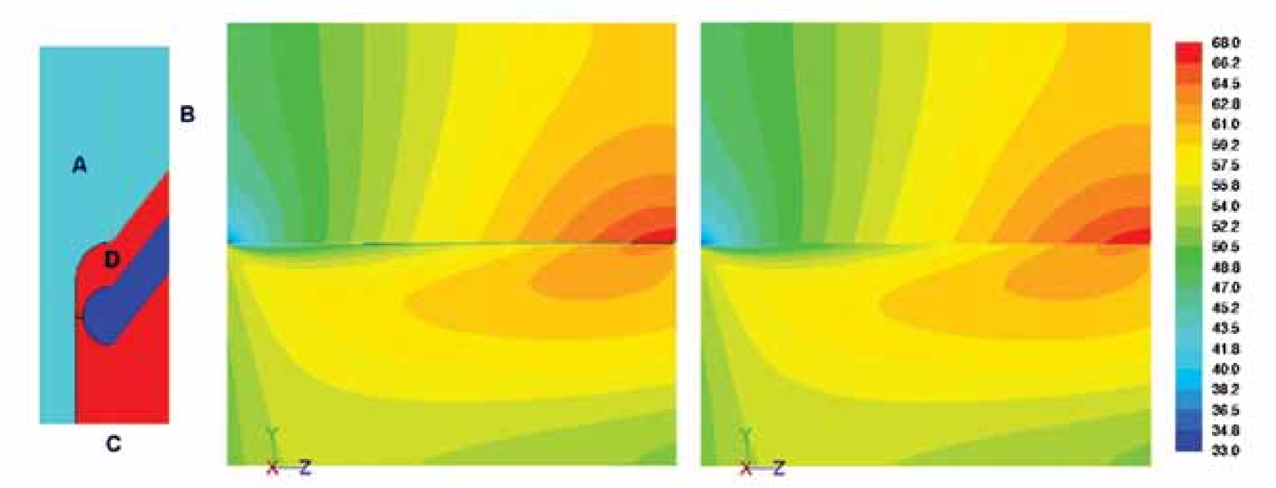

Figure 5. Simulation geometry and results. Left image: section of the computational geometry used for temperature modelling with Fluent temperature distribution (in °C) through vertical sections of the whole wafer (dark blue: wire; red: slurry; turquoise: Si-block/wafer). Middle image: midplane in the sawing channel. Right image: midplane through the wafer.

The aim of current research is to saw thinner wafers, be mindful of reducing kerf loss, while at the same time maintaining or even improving the wafer quality. The surface quality in particular has significant influence on the mechanical strength of the wafers, which becomes more important as the wafers get thinner.

Mounting of block before sawing

Prior to wafer sawing, silicon blocks are glued to a glass plate in contact with a metallic support (commonly made of aluminium or steel). During this process, the silicon brick is heated up to a predefined temperature (depending on glue properties) and then glued to the glass plate, which at the same time is glued to the metallic support. Afterwards the system cools down to room temperature. Through this series of events, thermal stresses develop in the regions in contact with the glue due to the differences in the coefficients of thermal expansion.

Finite element (FE) computations have been carried out to estimate thermal stresses introduced during the Si block gluing process (Fig. 4). Simulations have been performed to examine the effects of material properties of the glue: the initial temperature, the Young's modulus, the thickness of the glue layer and the effect of heat transfer conditions when the Si block was cooled down from 100 to 20°C. The simulations showed that tensile stresses were found in the vicinity of the block surface in contact with the glue. The main reason for the stresses developing is the difference in thermal contraction of the silicon block compared to the glue, glass plate and the support material.

The sawing process

Wafer quality is influenced by several parameters (e.g. wire speed and diameter, sawing velocity, and slurry properties). One important parameter is the temperature in the sawing zone. It is claimed that wafer warp and bow can be caused by undesirable temperature variation during the slicing [11,12]. The temperature variation will also influence the viscosity of the slurry and thus the flow conditions in the sawing gap. Slurry used in the wire sawing process consists normally of the organic liquid polyethylene glycol (PEG) mixed with silicon carbide abrasive particles. The viscosity of glycol can be seen to follow an Arrhenius dependence on temperature [13]. Also of note is that the slurry viscosity, η_s, is approximated well with corresponding temperature dependence as given in Equation 2 (temperature T expressed in Kelvin):

$$\eta_s = A\exp(T_E/T) \qquad (2)$$

The coefficients A and T_E will depend on the mean molecular weight of the PEG, the volume fraction of solid (SiC particles), and the particle size distribution. By using a value for the temperature constant in Equation 2 of T_E = 3500K, we can calculate the ratio of the viscosity at different temperatures related to the viscosity at an initial temperature T_i (i.e., the inlet temperature of the slurry). In quantifying the temperature variation, it was decided to perform temperature measurements and heat modelling of the silicon block/wafer, including the slurry and the wire. As will be seen in the following section, the temperature variation led to a significant slurry viscosity variation within the sawing gap. Whether this also significantly affects the distance between the wire and the silicon block and thereby the material removal rate is not yet clear and is currently undergoing research.

Saw parameter	Value
Wire speed	14 m/s
Wire diameter	120µm
Wafer thickness	150µm
Width of sawing cut	150µm

Table 1. Sawing parameters.

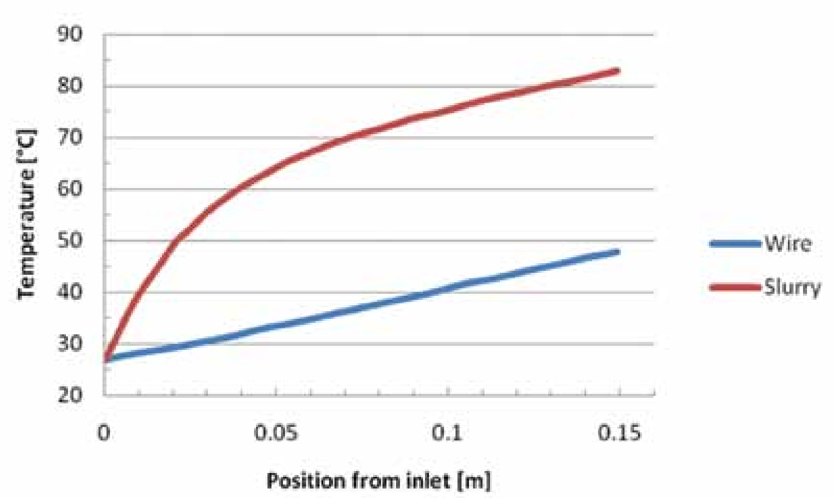

Figure 6. Profile of temperature in wire (centre) and slurry. The slurry temperature is taken in the midplane of the wire halfway between the wire and silicon surface.

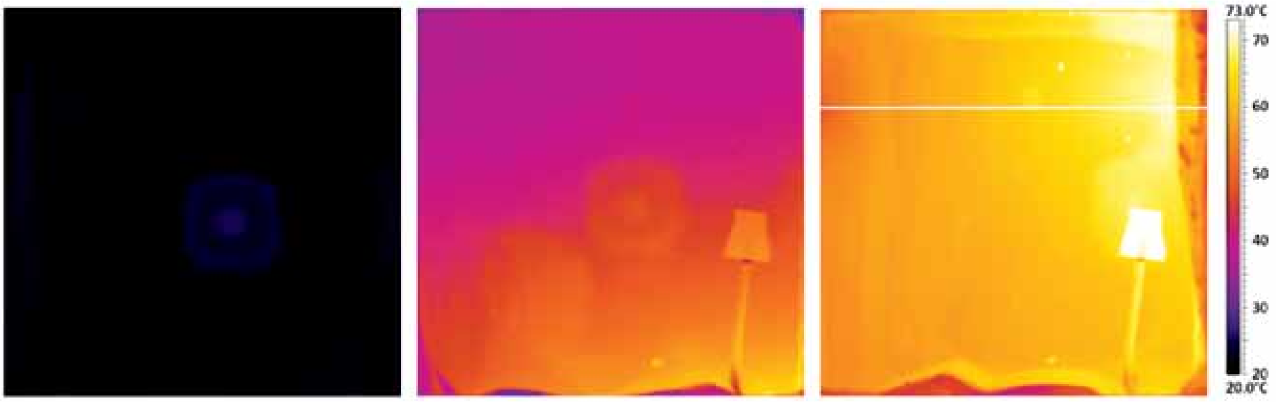

Figure 7. Full-field thermal image of the front surface of the block. An approximately 5mm area at the wire entrance and wire exit are shielded by the splash protection. Left image: a block at room temperature before sawing. The reflection from the camera is visible in the centre of the image. Middle image: temperature field at about 2mm table progress after wire/block contact. A temperature point sensor can be seen at the right of the image. Right image: temperature field at the end of the sawing process. The sawing front is indicated by the white horizontal line [14].

The following two sections present temperature measurements and heat modelling of a multicrystalline silicon block during wafer sawing. Table 1 specifies the sawing parameters used for the measurements and modelling.

Temperature modelling

The differential equation for heat conduction and convection is solved simultaneously in the silicon block, slurry and wire with the use of the computational fluid dynamics (CFD) code Fluent. End effects at the block top and bottom are neglected and symmetry is assumed between wafers. In this way, the three-dimensional geometry is confined to a volume consisting of half of the thickness of the wafer below the wire and halfway into the sawing channel. The whole wafer/block is included in the wire and sawing direction (Fig. 5).

To avoid a complicated free-surface flow problem we anticipate that the sawing channel is filled with slurry. The power supplied to the wire saw machine is partly used to remove silicon kerf from the block, while most of the power ends up as friction heat in the gap volume between the wire and the silicon surface. In the simulations depicted in Fig. 5, a power source of 10W is specified for the slurry in the region D (left-hand image). The temperature at inlet for slurry and wire is set to 300K. On the boundaries Inlet A, Outlet B and Bottom C, the heat flux is specified to be proportional to the temperature difference between the surface and the surrounding medium.

Taking a large view of the whole wafer, there seem to be only minor differences between temperatures in a midplane in the wafer compared to a midplane in the sawing channel (Fig. 5). A more close-up view is needed to reveal the local temperature variations. The graph in Fig. 6 shows how the temperature increases in the wire and slurry in the wire direction.

Temperature measurements

Temperature measurements can be carried out with an IR-camera. This is a non-contact technique and thus does not influence the process. In-situ measurements can be performed by installing a splash protection and investigating the polished front surface of the block. Furthermore, IR-camera measurements give full field information about the absolute temperature distribution of the block surface. To obtain absolute measurements it is necessary to develop a good model of the emissivity of the different regions of the block [14].

Fig. 7 shows the compensated temperature field measurements at different stages of the sawing process. The left image shows the temperature distribution before starting the saw run when the whole block is at room temperature. The temperature field in the centre image was recorded in the beginning of the saw run after about 6 minutes. This corresponds to a table progress of about 3mm after contact is made between the wire and the block. The wire has barely entered the block and is hidden behind the splash protection. It can be seen that the temperature increases rapidly when the wire starts to saw. After just 6 minutes, a maximum temperature of 60°C is obtained, but the temperature increases only slightly when the sawing process progresses.

In the right-hand image in Fig. 7, a maximum temperature of about 70°C can be seen. However, the block temperature depends on the saw parameters. Friction force increases slightly with wire speed [15] and so friction heat generation is about proportional to wire speed. A higher wire speed will therefore contribute strongly to increase the temperature. Slurry viscosity and the table speed also influence the absolute temperature.

Discussion

The presented temperature measurements verify the modelling of the temperature field. The temperature gradients during wafer sawing can contribute to deviations in several wafer quality parameters [11]. The temperature variation from the start of the saw run until the maximum temperature is reached can be estimated at about 50°C, while the temperature difference from wire entrance to wire exit after reaching stable sawing conditions is about 20°C. This leads to thermal expansion-induced shape deviations in the wafer. From the experiments, we know that the thermal conditions are almost stable after 20 minutes corresponding to a change of typically 4-8mm in table position.

Based on the coefficient of thermal expansion for Si ($\alpha_L = 2.6 \cdot 10^{-6}$ K^{-1}) and assuming unrestricted expansion of the block, an estimation for the warp and bow can be calculated. The resulting warp will be a maximum of 6.5µm. This will be superimposed on a bow of maximum 16.5µm relative to the centre wafer of the block. These shape deviations are in the range of a typical saw mark criterion for an A-wafer.

A more complex model is needed to calculate the total influence of thermal expansion taking into account the glass plate, the metal support and the thermal conditions in the saw, in particular the thermal expansion of the wire guides.

However, the most critical parameter is the change in the slurry properties. The heat is generated in the sawing channel. If the temperature increases the viscosity of the slurry will be decreased; thus, the slurry properties are significantly changed along the saw channel, which will influence the quality of the sawing process.

Conclusions

The production control of Si wafers is currently moving from a mainly empirical towards a more scientifically-based approach, which naturally requires more detailed knowledge about the processes. In this context, advanced temperature measurement techniques and the development and use of simulation tools become increasingly important.

There is a huge body of work dedicated to the study of crystallization processes and in particular to the Cz process. It is now well established that control of the thermal field, crystallization conditions and melt flow is essential for ingot quality. Dedicated simulation tools for the silicon crystallization process are now available and increasingly used by the industry to analyse and optimize the process. These requirements are in turn pushing the modelling community towards a more refined description of the process including e.g. impurity transfer with the furnace atmosphere, advanced melt flow models and grain structure predictions. The use of heat transfer models for inline control of the processes is still limited. There is, however, a growing trend towards physically-based PID controllers.

The study of the influence of temperature variations on subsequent processes is the topic of more recent research. Sawing parameters dictate the temperature field during wafer sawing. The results presented here show a typical temperature difference of more than 20°C from the wire entrance to the wire exit, with a measured maximum temperature of the Si block of about 70°C. The temperature gradients influence the warp and bow parameters of the produced wafers. Furthermore, the change in slurry viscosity is introduced as a critical parameter. The presented temperature measurements verify the models to a large degree.

Acknowledgements

The authors acknowledge REC Wafer AS for supplying the mc-silicon block and Washington Mills AS for supplying SiC for the slurry in the sawing experiments. The authors thank **Prof. H.J. Möller** and **R. Ritzschel** from TÜ Bergakademie Freiberg for providing the multi-wire saw and the support during the temperature measurements and **X. Ma** and **S. Gouttebroze** for providing the results of Figure 4. Some of the results presented in this work have been carried out in projects funded by REC Wafer AS, Elkem Solar AS and NorSun AS. Support from the industrial partners and the Norwegian Research Council is greatly acknowledged.

References

[1] Meese, E.A., Øvrelid, E.J., Laux, H. & M'Hamdi, M. 2005, "Advanced heat transfer modelling of a furnace for directional growth of multicrystalline silicon", *Proc. 20th EU PVSEC*, Barcelona, Spain, paper 2CV.4.44.

[2] Jomaa, M., M'Hamdi, M., Nielsen, Ø. & Park, G.-S. 2009, "Numerical Study of the Continuous Czochralski Process for Silicon Crystal Growth", *Proc. 24th EU PVSEC*, Hamburg, Germany, pp. 1273–1276.

[3] Fujiwara, K., Obinata, Y., Ujihara, T., Usami, N., Sazaki, G. & Nakajima, K. 2004, "Grain growth behaviors of polycrystalline silicon during melt growth processes", *J. Crys Growth*, 266, pp. 441-448.

[4] Di Sabatino, M., Juel, M., Arnberg, L., Syvertsen, M. & Tranell, G. 2009, "Control of grain size and orientation in multi-crystalline silicon ingots", *Transactions of the Indian Inst. of Metals*, 62, 4-5, pp. 511-513.

[5] Vizman, D., Friedrich, J. & Mueller, G. 2007, "3D time-dependent numerical study of the influence of the melt flow on the interface shape in a silicon ingot casting process", *J. Crystal growth*, 303, 1, pp. 231-235.

[6] Liu, L. & Kakimoto, K. 2005, "3D global analysis of CZ–Si growth in a transverse magnetic field with various crystal growth rates", *J. of Crystal Growth*, 275, 1-2, pp. e1521-e1526.

[7] Laux, H., Meese, E.A., Øvrelid, E.J. & M'Hamdi, M. 2005, "Modelling of solute transport during directional solidification of multicrystalline silicon", *Proc. 20th EU PVSEC*, Barcelona, Spain.

[8] M'Hamdi, M., Meese, E.A., Laux, H. & Øvrelid, E.J. 2006, "Thermo-mechanical Analysis of Directional Crystallization of multi-crystalline silicon ingots", *Mater. Sci. Forum*, 508, pp. 597-602.

[9] Bhagavat, M., Prasad, V. & Kao, I. 2000, "Elasto-Hydrodynamic Interaction in the Free Abrasive Wafer Slicing Using a Wiresaw: Modelling and Finite Element Analysis", *Trans ASME J Tribology*, 122, pp. 394-404.

[10] Möller, H.J. 2006, "Wafering of silicon crystals", *Phys. Stat. Sol.* (a), 203 (4), pp 659-669.

[11] Yamada, T., Fukunaga, M., Ichikawa, T., Furuno, K., Makino, K. & Yokoyama, A. 2002, "Prediction of Warping in Silicon Wafer Slicing with Wire-Saw Machine", *Theoretical and Applied Mechanics*, 51, pp. 251-258.

[12] Bhagavat, S. & Kao, I. 2008, "A finite element analysis of temperature variation in silicon wafers during wiresaw slicing", *Int J Machine Tools & Manufacture*, 48, pp. 95-106.

[13] Incropera, F.P. & DeWitt, D.P. 1996, *Fundamentals of Heat and Mass Transfer*, 4th ed, J. Wiley & Sons.

[14] Johnsen, L., Gastinger, K., Bjerkan, L., Rietzschel, R. & Möller, H.J. 2009, "Absolute Temperature Measurements in Wire Sawing Process", *Proc. 24th EU PVSEC*, Hamburg, Germany.

[15] Rietzschel, R., Wagner, T., Funke, C. & Möller, H.J. 2008, "Optimization of the wire sawing process using force- and temperature-measurements", *Proc. 23rd EU PVSEC*, Valencia, Spain.

About the Authors

Kay Gastinger did his Master's degree in 1997 on electrical engineering at the Technical University of Ilmenau, Germany. He received his Ph.D. in 2006 in physics within the field of interferometry from the University of Oldenburg, Germany. He joined SINTEF in Trondheim, Norway in 1997 and works there as a senior scientist in the Department of Optical Metrology and Data Analysis. His main areas of expertise are optical metrology, in particular interferometry, and micro optics. His current focus is on in-line and off-line inspection systems for solar cell production.

Mohammed M'Hamdi is a senior scientist with SINTEF Materials and Chemistry, Department of Metallurgy in Oslo, Norway. He is also Adjunct Professor with the Norwegian University for Science and Technology (NTNU) in Trondheim, Norway. He has been working with the development of mathematical modelling tools for solidification processes for about 16 years. His current research includes modeling of silicon crystal growth processes as well as the solidification of aluminium alloys.

Trond Bergstrøm studied physics at the Norwegian Institute of Technology (NTH) and later received his Ph.D. degree in process metallurgy (1988). He is now working as a senior scientist in SINTEF Materials and Chemistry, Department of Metallurgy in Trondheim, Norway. He has been working mainly in the field of modelling of metallurgical processes. In recent years, his work on silicon for PV applications has focused on wire sawing and handling of wafers.

Lars Johnsen received his M.Sc. in electrical engineering/physical electronics from the Norwegian Institute of Technology (NTH) in 1986. He joined SINTEF in 1989 and is currently working as a scientist in the Department of Optical Metrology and Data Analysis. His main fields of work have been semiconductor materials and circuit fabrication, optical sensor systems and optical measurement technology. His current focus is on optical metrology for in-line and off-line inspection of wafer-based Si solar cells.

Enquiries

SINTEF
7465 Trondheim
Norway

Email: kay.gastinger@sintef.no